2

Spine Anatomy

John M. Mathis

Percutaneous vertebroplasty (PV), kyphoplasty (KP), and percutaneous sacroplasty (PS) require accurate localization of the bone region to be treated and careful identification of the trajectory that must be followed for safe device insertion. The normal anatomic structures and pathologic factors that affect the spine must be understood to accomplish this goal. This chapter describes the pertinent anatomy of the spine for these image-guided procedures and discusses how special variations or situations can affect the choice of devices and appropriate needle trajectories.

General Spine Anatomy

The spine is made up of 33 bones: 24 vertebrae consisting of 7 cervical, 12 thoracic, and 5 lumbar elements. The sacrum and coccyx provide unique variations. The sacrum is composed of 5 segments that are fused. The coccyx has 4 segments that are variably fused (1).

The multiple spine segments are joined by intervening discs and structurally augmented by connecting ligaments and muscles. The entire spine is depicted in Figure 2.1A, demonstrating the natural curvature that changes from segment to segment. Viewed from the lateral projection, there is normally lordosis in the cervical and lumbar segments and mild kyphosis in the thoracic and sacral regions. These variations in curvature are important as they affect the orientation of the individual vertebra and critical vertebral components like the pedicles that are commonly used for device access to the vertebral body in PV and KP (Figure 2.1B).

The vertebrae progressively enlarge from the cervical through the lumbar region. There is also variability in vertebra size at any particular level based on the individual's size. For instance, an upper thoracic vertebra in a small woman may have a diameter of only 2–2.5 cm (similar to a U.S. quarter). A large male may have a vertebra at the same level that is one to two times larger. These variations in size affect the initial volume of each vertebra, which will ultimately affect the amount

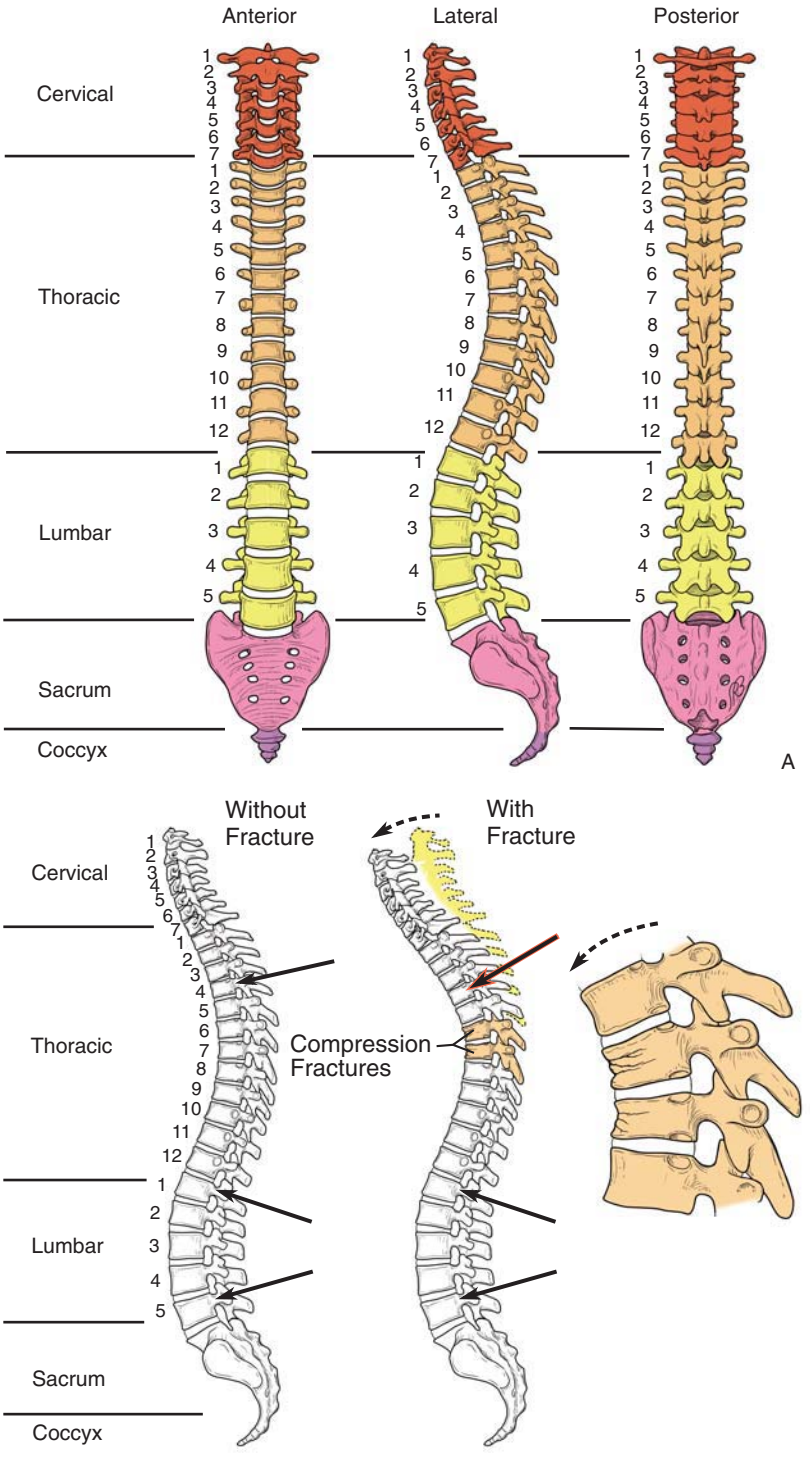

Figure 2.1. (A) AP, lateral and posterior depictions of the entire spine. The lateral view shows the normal lordotic curve found in the cervical and lumbar regions. A kyphotic curve is normal in thoracic and sacral regions. These curves can be modified or accentuated in disease. **(B)** Drawing to show how the usual transpedicular needle entry angle (black arrows) changes as vertebrae experience compression deformity and kyphosis increases in the thoracic spine. Increasing kyphosis occurs with compression fractures of the thoracic spine (dashed arrow).

of cement that can be used safely to augment a fracture without overfilling. Variations in vertebral volume are also affected by the amount of collapse a vertebra has experienced during fracture. The original and ultimate (postcollapse) sizes of the vertebra are of extreme importance when one is performing PV or KP. In both procedures, the most common side effects are created by cement leaks (2). This results from natural and pathologic holes in the vertebra as well as overfilling.

To avoid overfilling it is important to appreciate the general volume range of vertebral bodies between the cervical and lumbar regions and the effect that compression has on the initial volumes (Table 2.1). Using volumes computed for a hollow cylinder (and with representative dimensions taken for vertebrae in the cervical, thoracic, and lumbar regions), we find initial theoretical volumes ranging from 7.2 mL in the cervical spine (C5) to 22.4 mL in the lumbar spine (L3). Both larger and smaller vertebrae may be present. Because of the thickness of cortical and trabecular bone, the fillable volume is on the order of 50% or less of the theoretical volume. The fillable volume will again be diminished by the amount of collapse experienced during the compression fracture. As shown in Table 2.1, the 50% compressed, *fillable* volume of C5 is estimated at 1.8 mL. In the thoracic spine at T9 the 50% compressed volume estimate is 3.8 mL. At L3 the 50% compressed volume estimate is 5.6 mL. Actual cement volumes used to augment these vertebrae may be even less. This shows that quite small volumes will be needed to biomechanically augment a vertebra after fracture and that larger volumes will simply lead to overfilling and cement leak.

The vertebrae vary in size, with the smallest vertebra found in the cervical area and the largest in the lumbar. Size variation at a particular level is also common and is based on sex and general body dimensions.

Cervical Spine

The cervical spine (Figure 2.2) contains seven segments that vary tremendously in configuration from top to bottom (3). The first cervical vertebra is unique, and little actual distinct vertebral body exists at this level. Opportunities for percutaneous cement augmentation, therefore, are limited, as the body of the vertebra is the target for this type of therapy. Percutaneous vertebroplasty has been performed in all other cervical vertebrae, with the pathologic cause almost always being

Table 2.1. Vertebral volume estimates from cervical to lumbar spine.

Vertebral Level	Theoretical Volume (mL)	Fillable Volume (mL)	50% Compressed Volume (mL)
C5	7.2	3.6	1.8
T9	15.3	7.65	3.8
L3	22.4	11.2	5.6

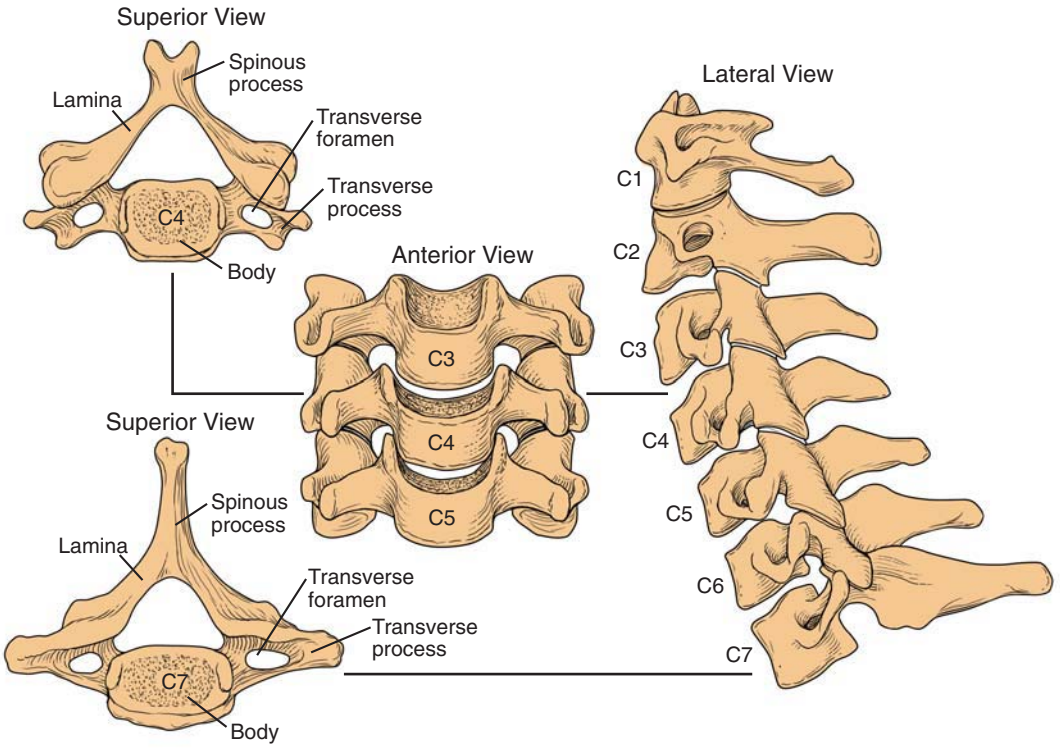

Figure 2.2. The cervical spine and vertebrae.

some form of neoplastic destruction with a subsequent compression fracture. Osteoporotic fractures are rare in the cervical spine.

The most common approach to the cervical spine for percutaneous bone augmentation has been via the anterolateral approach. This usually requires an accompanying manual maneuver that transiently displaces the carotid–jugular complex out of the way while a guide or primary needle is inserted into the margin of the vertebral body (Figure 2.3). The right side is chosen to avoid the needle transiting the esophagus (which lies behind or to the left of the trachea). The angle of the mandible can make access to high cervical vertebra, particularly C2, difficult. An occasional procedure has been performed via a trans-oral approach (4). The angle in this situation is improved by going through the mouth, but one cannot eliminate the added risk of trans-oral contamination of bacteria. For this reason, this route must not be considered optimum at C2. The lateral approach has also been used and is not optimum because of the potential for injury to the vertebral artery, which is fixed along the lateral aspect of the vertebral body (Figure 2.4). At C2–C6 the vertebral artery courses through the foramen transversarium and cannot be displaced as can the carotid–jugular complex during needle insertion. Regardless of the needle approach, computed

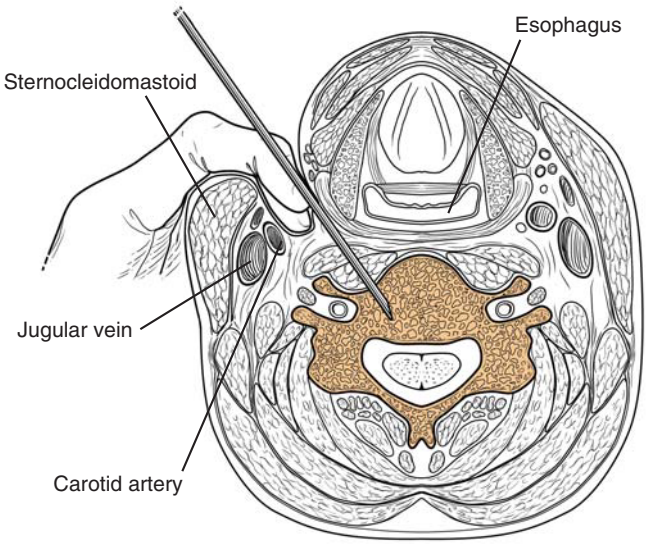

Figure 2.3. Anterior cervical approach. Axial drawing demonstrates manual displacement of the carotid–jugular complex during needle introduction. Note that the right side is chosen to best avoid the esophagus (as is the case with discography).

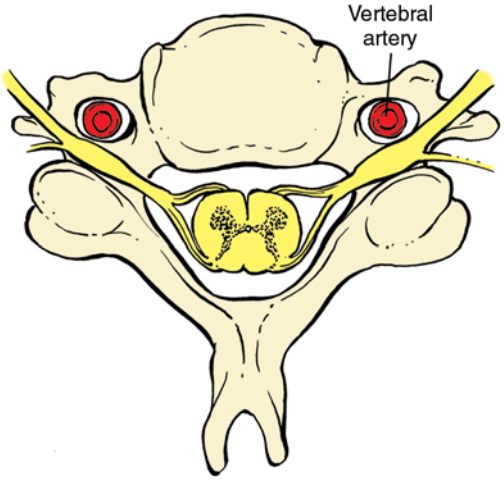

Figure 2.4. Drawing of a cervical vertebral body shows the position of the vertebral artery along the lateral aspect of the vertebral body in the foramina transversarium. A lateral needle approach would put the vertebral artery at risk. (From Mathis [2], with permission).

tomography (CT) offers an accurate method of visualizing structure that must be avoided during needle introduction.

Thoracic Spine

The thoracic spine is made up of 12 thoracic vertebra aligned with a gentle kyphosis in the normal, healthy spine. There is less variation in vertebral shape from top to bottom here than in the cervical region. Size variation is considerable and amounts to approximately a factor of 2 from T1 to T12. All thoracic vertebrae have a junction with a rib on each side, with ligaments attaching the rib head to the vertebral body and the adjacent rib to the vertebral transverse process (Figure 2.5). Just as there is substantial variation in the size of the thoracic vertebrae from top to bottom, there is considerable variation in the size and orientation of the pedicles as well (5). Pedicles at the lower aspect of the thoracic spine are relatively large and oriented in almost a direct anteroposterior (AP) direction (Figure 2.6A). Ascending toward the upper thoracic spine there is a progressive decrease in the size of the pedicles. Orientation remains AP until the most superior thoracic vertebrae (T1 and T2). The uppermost thoracic vertebrae have a more obliquely oriented pedicle (Figure 2.6B).

The vertebrae have a convex anterior margin and concave posterior margin when viewed from above (Figure 2.6). This is important, as

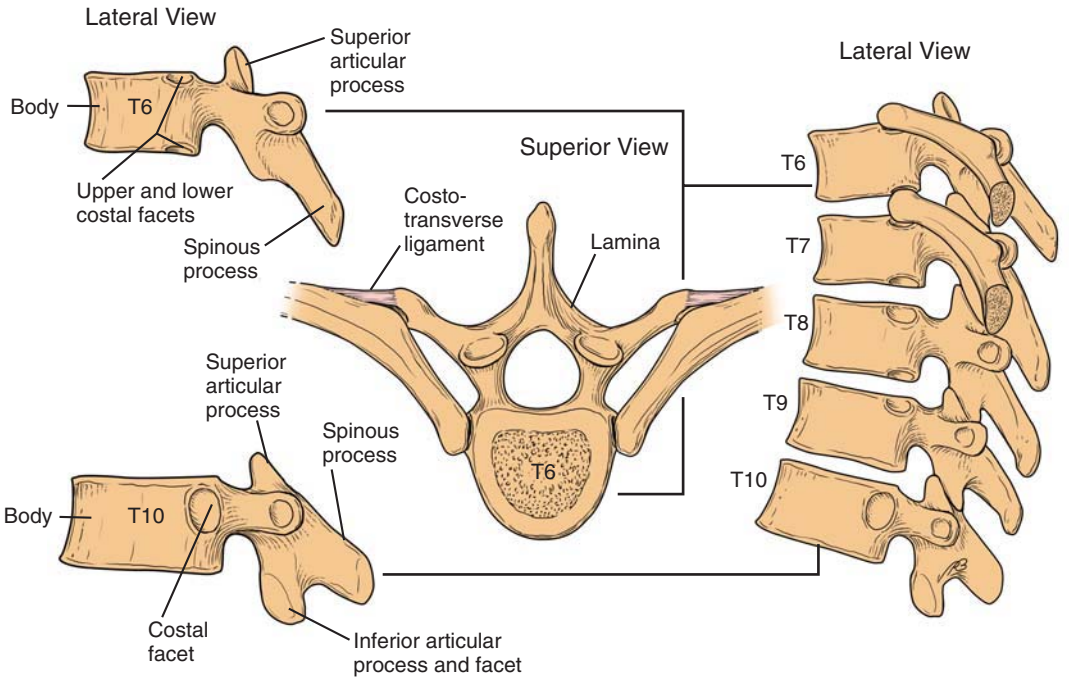

Figure 2.5. Artist's depiction of the thoracic vertebrae. There is considerable change in vertebral size from T1 to T12.

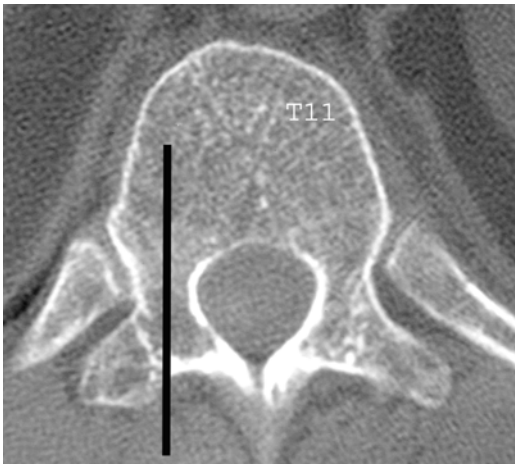

A

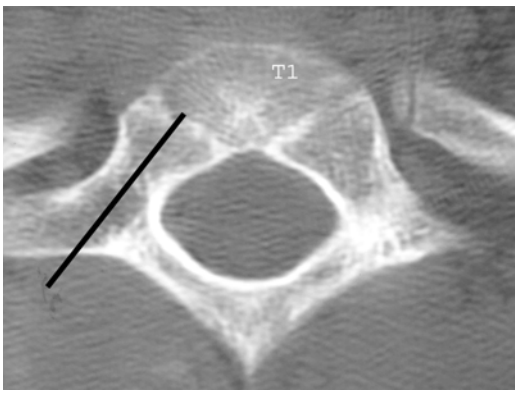

B

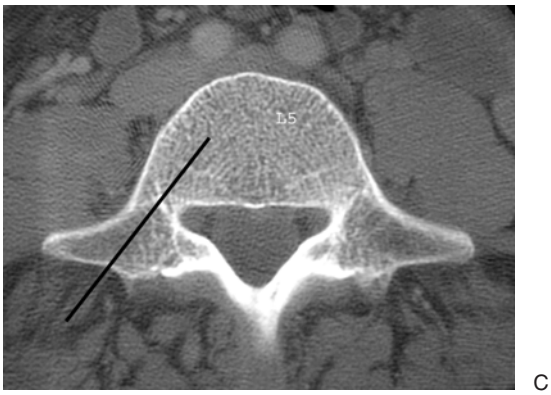

C

Figure 2.6. (A) The T11 vertebra is shown. The transpedicular angle is essentially straight in the anterior to posterior direction. The black line shows the angle and the needle direction that a transpedicular approach will take. All vertebrae from about T3 to L3 have a similar transpedicular angle. **(B)** This is the T1 level. Note the large change in the transpedicular angle compared with T11 (above). A transpedicular approach will have a much more lateral to medial approach (black line). **(C)** This level is L5. The high thoracic and lowest lumbar vertebrae show the most extreme transpedicular angles (away from AP).

lateral observation during fluoroscopy only depicts the extreme anterior and posterior dimensions. Cement will exit the curved posterior wall before getting to the apparent posterior limit as seen with fluoroscopy (Figure 2.7A,B). Likewise, placing a needle through a straight AP pedicle orientation will result in a lateral needle position that can breech the anterolateral wall before reaching the apparent anterior limit, as shown in the lateral projection (Figure 2.7C).

The needle approach to the T3–T12 thoracic spine is either transpedicular (through the pedicle) or parapedicular (transcostovertebral)

Figure 2.7. (A) A lateral radiograph after PV demonstrates the apparent anterior and posterior vertebral margins (black arrowheads). Cement in the back of the vertebra (white arrow) appears to stop before reaching the posterior vertebral margin. **(B)** Computed tomography scan of the same vertebra as in A. Note the concave posterior margin of the vertebra and the small cement leak (white arrow). The actual vertebral margin ends before the apparent margin as seen on the lateral radiograph. Cement injection should be stopped when cement enters the posterior quarter of the vertebra. **(C)** An axial CT scan of a thoracic vertebra demonstrates its very convex anterior margin. The black line depicts a straight transpedicular approach. Note that this approach would breach the anterior cortex long before the needle reaches the apparent anterior margin when seen in the lateral projection.

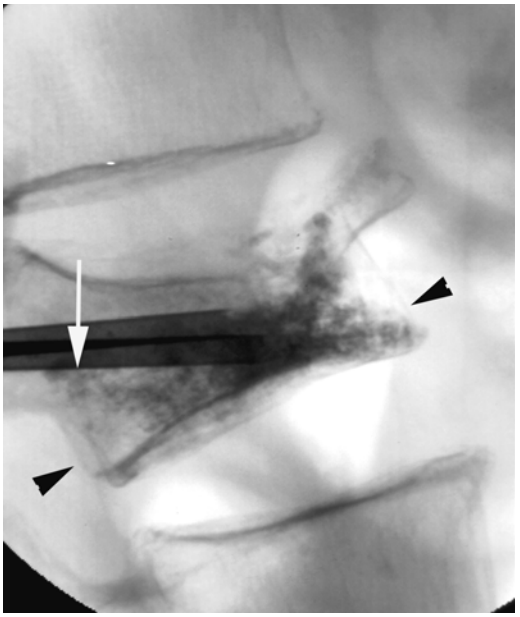

A

B

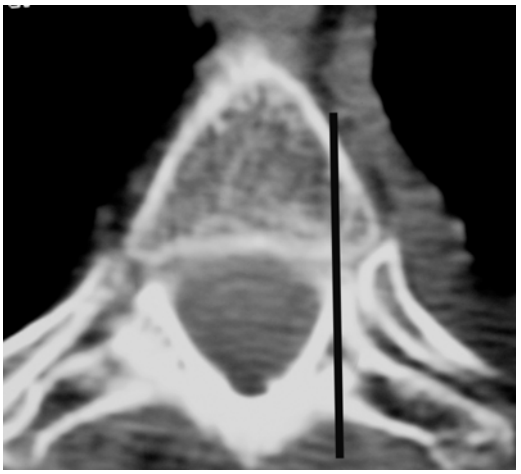

C

(6,7,8) through the junction of the rib and transverse process. The transpedicular approach (Figure 2.8A) is the most commonly used and safest, but small pedicle size may make it difficult to use large-bore needles (10–11 gauge). Reducing needle size to 13 gauge will eliminate this problem in adults regardless of thoracic level. The parapedicular approach (Figure 2.8B,C) allows placement of a needle above the transverse process and lateral to the pedicle. This has been found useful for larger instruments (commonly used in KP) or when the pedicle is destroyed or not adequately visualized because of severe osteoporosis. It is not recommended as the primary access method because of its higher potential complication rate related to either pneumothorax or hemorrhage.

The upper thoracic spine (T1–T2) can also be approached via the anterolateral method described for the cervical region (9,10,11). This transitional region has similarities of both the cervical and thoracic spine that allows these options. Pedicle orientation differences at these levels must be considered if a transpedicular approach is used (see Figure 2.6B).

Lumbar Spine

There are five lumbar vertebrae that make up the largest of the vertebrae found in the spine (Figure 2.9). These vertebrae have mild size variations from L1 to L5 (8). Pedicle orientation is quite different from L1 to L5. The pedicles of the upper lumbar region are similar to the lower thoracic with a nearly straight AP orientation. This gradually becomes a more oblique angle toward the lower lumbar spine and is maximal at L5 (see Figure 2.6C).

The approach to the lumbar spine for PV or KP is almost always transpedicular (see Figure 2.8A). The pedicles of the lumbar spine are large and allow access in most adults with 10–11 gauge needles without difficulty. The parapedicular (Figure 2.8B,C) approach remains a viable option but is much less needed because of the generous pedicle size in this region. The posterolateral approach is of historical value only (a low approach below the transverse process that places the exiting nerve root at risk of injury) and used only by manufactures' of instruments that are large and not required for the standard, minimally invasive procedure of PV or KP.

Sacrum

The sacrum (and coccyx) forms the terminal end of the lower spine. It is composed of five segments that are fused (Figure 2.10A). The lower lumbar spine joins the sacrum from above through the L5–S1 disc, making an articulation similar to other intervertebral junctions. The sacrum is joined to the pelvis via the sacroiliac (SI) joints. It is shaped like a "keystone," tapering to a narrower transverse width along its inferior margin (Figure 2.10B). This aids weight transfer to the pelvis without allowing slippage between the sacrum and pelvis through the SI joints. However, this anatomic shape and junction at the SI joints

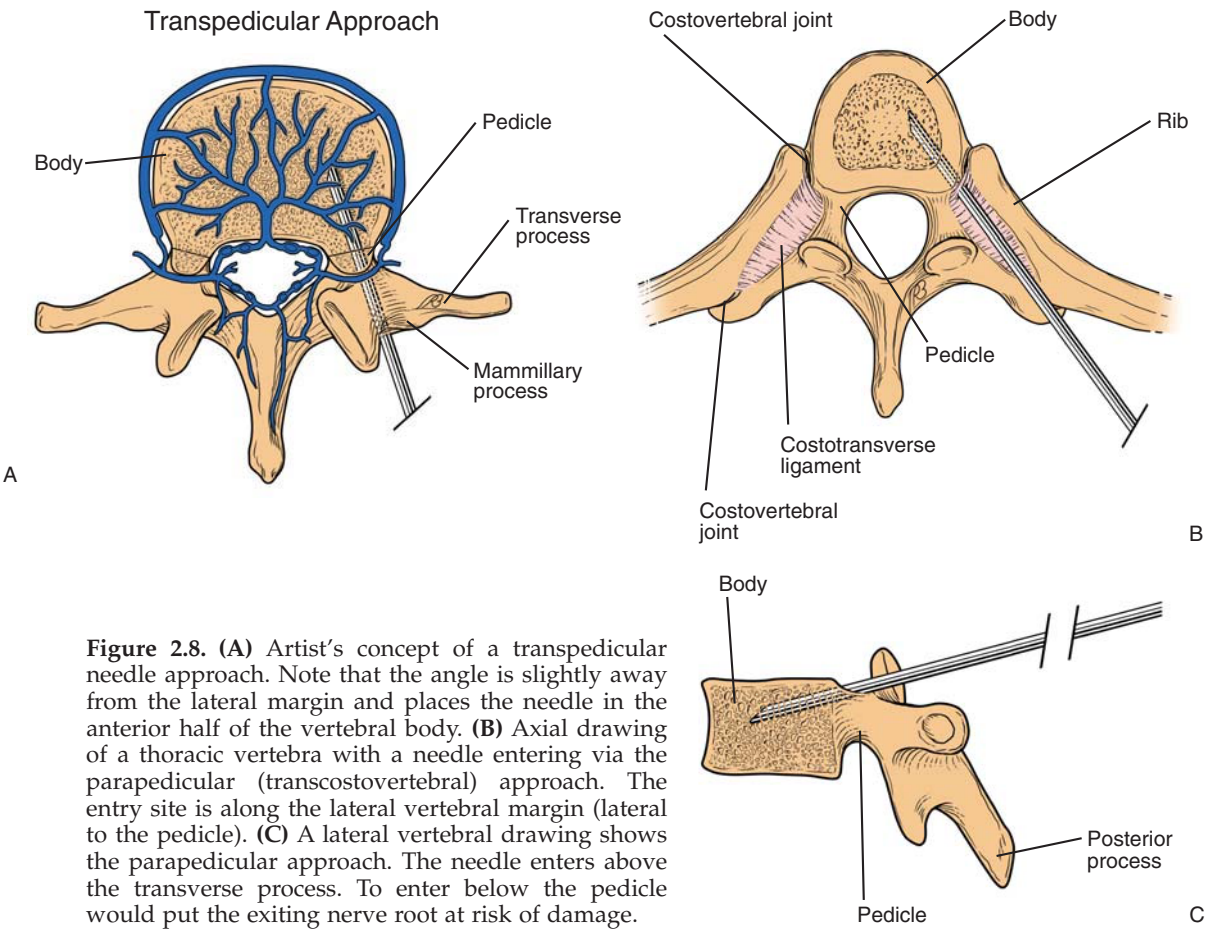

Figure 2.8. (A) Artist's concept of a transpedicular needle approach. Note that the angle is slightly away from the lateral margin and places the needle in the anterior half of the vertebral body. **(B)** Axial drawing of a thoracic vertebra with a needle entering via the parapedicular (transcostovertebral) approach. The entry site is along the lateral vertebral margin (lateral to the pedicle). **(C)** A lateral vertebral drawing shows the parapedicular approach. The needle enters above the transverse process. To enter below the pedicle would put the exiting nerve root at risk of damage.

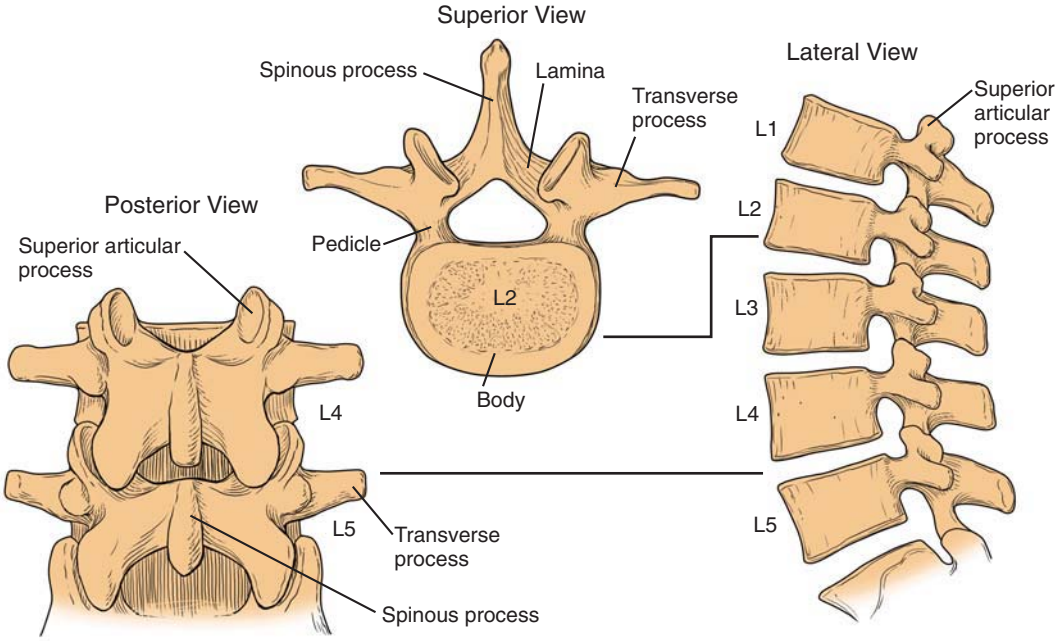

Figure 2.9. The lumbar vertebrae.

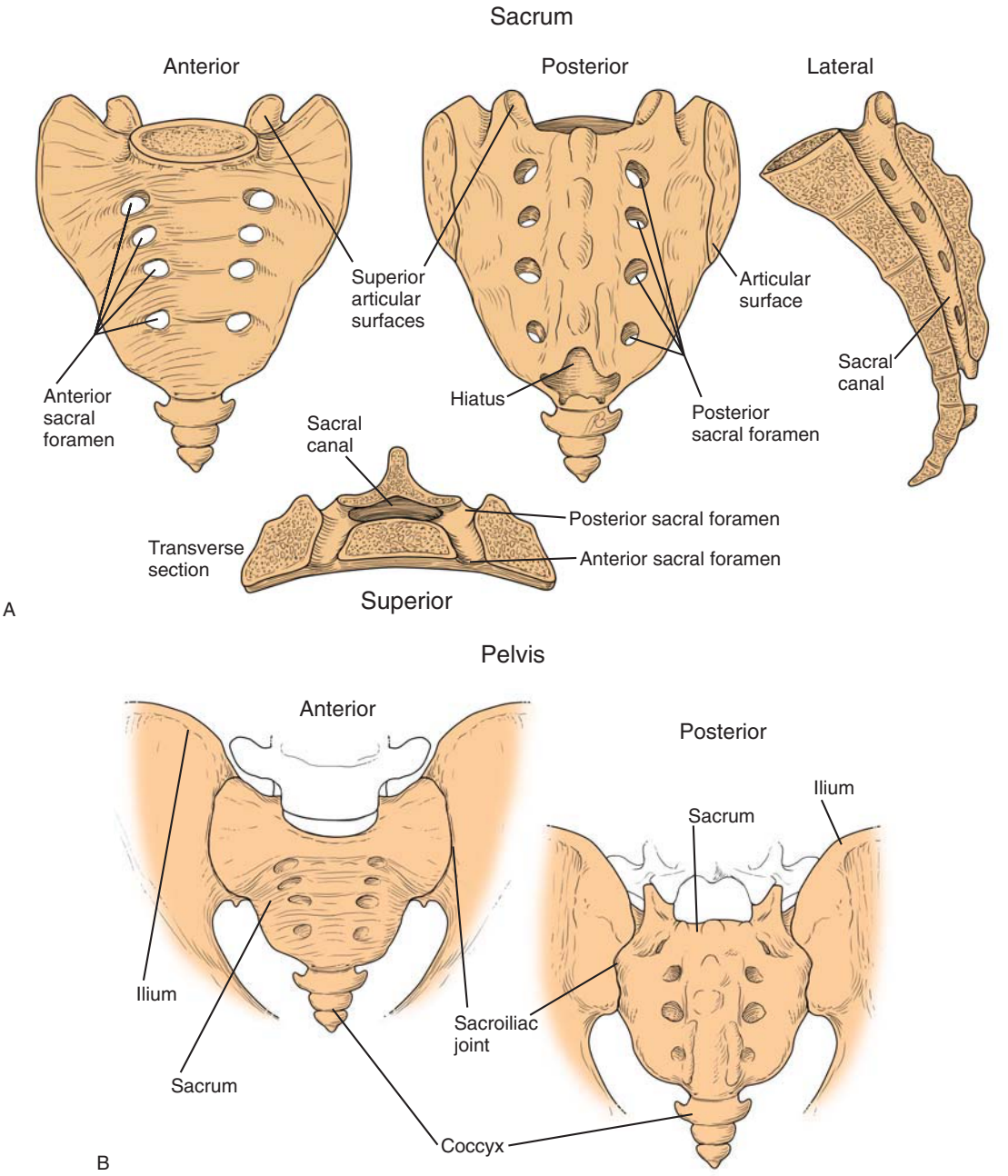

Figure 2.10. (A) Multiple views of the sacrum and coccyx. **(B)** Drawing demonstrates the association of the sacrum and pelvic bones. The sacrum forms a "keystone" within the pelvic ring. This "keystone" configuration acts to keep the sacrum from slipping downward with pressure from above. When the sacrum yields during a sacral insufficiency fracture, the lateral sacral wings (ala) give way and fracture parallel to the sacroiliac joints.

does create the unique fractures seen in the sacrum due to osteoporosis and trauma (see below).

Sacral insufficiency fractures may be percutaneously augmented to relieve pain such as compressed vertebrae. However, needle access is different because of the unique anatomic structure of the sacrum (compared with the vertebrae) and the different configuration of the fractures. Access to the sacral wings is usually from a posterior-oblique approach (Figure 2.11). This will require two needles if there is a bilateral sacral wing fracture. If the fracture extends into the central body of the sacrum, a needle approach through the SI joint or between the spinal canal and foramina may be necessary.

The size of the sacrum is large compared with a single vertebra, and therefore cement augmentation usually requires considerably more cement for similar filling of the fracture region.

Vascular Anatomy

The arterial supply to the vertebral bodies comes from arterial branches that leave the aorta and run along the lateral margins of the vertebrae supplying the vertebral body, the epidural space, and exiting nerve roots (Figure 2.12) (2,9). Communications between these branches exist up and down the paraspinous region. Supply to the spinal cord is intermittent and not dependably found at any one level.

Three interconnecting, valveless venous systems (interosseous, epidural, and paravertebral) make up the vertebral venous supply (1).

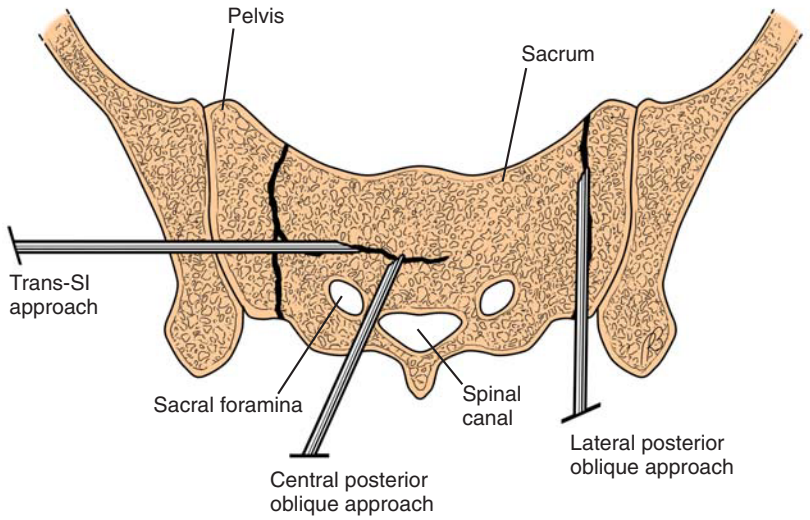

Figure 2.11. This drawing demonstrates the various needle angles that can be used to access the fractures of a sacral insufficiency fracture. The most common is the posterolateral that parallels the sacroiliac joint.

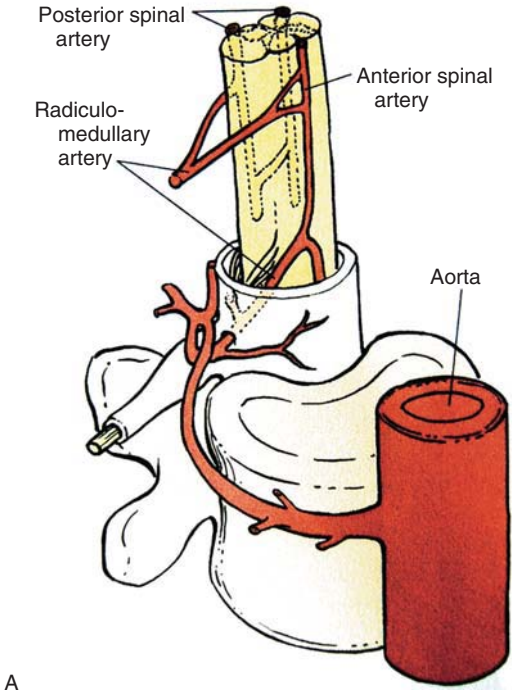

A

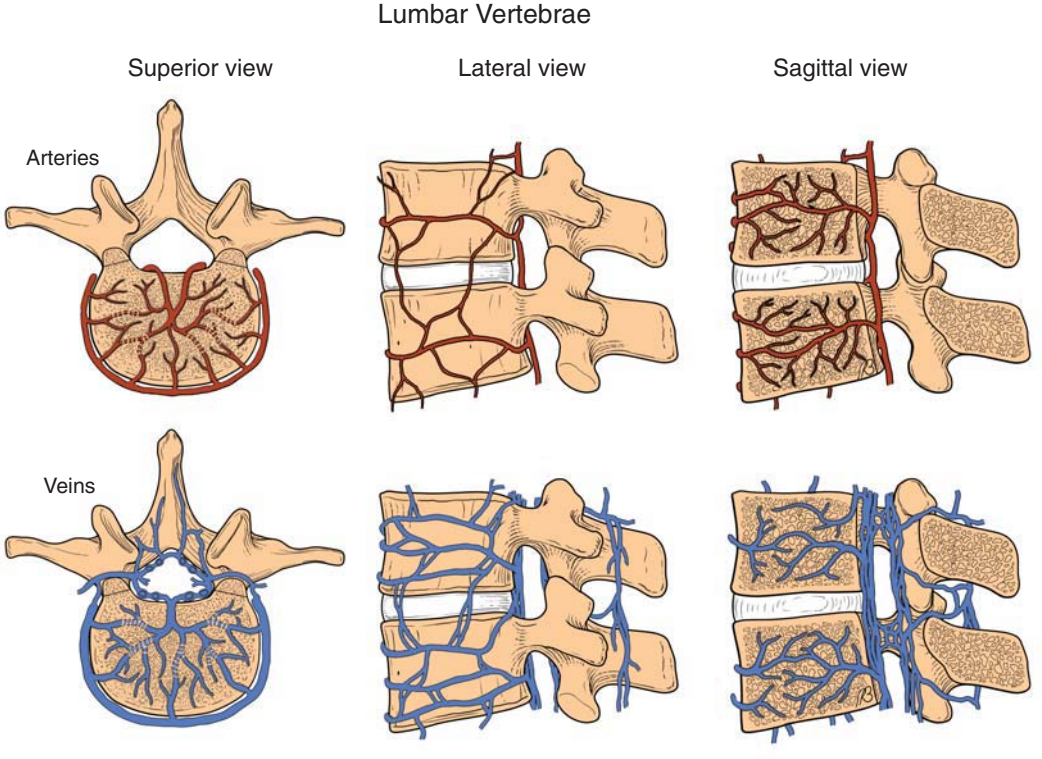

B

Figure 2.12. (A) Drawing of the aortic arterial branch that supplies the vertebral body and gives branches into the foramina and ultimately to the spinal cord. The cord supply is variable at each segment. The branches are found bilaterally. **(B)** Multiple projections of the arterial and venous supply to the vertebral bodies and epidural space. The venous elements are more numerous at all levels compared with the arteries. (A, from Mathis [2], with permission).

Through these systems there is intimate communication with the intraosseous, intertrabecular space (Figure 2.12B). Blood products and marrow fat are harbored in this space and commingled with flowing blood at venous pressure. This space in the axial skeleton becomes a primary source of blood-forming elements in the older adult. It is this space into which the cement is injected during PV or KP. Communication of the intertrabecular space via connecting venous systems can allow potential posterior, lateral, or anterior cement leaks to occur. Posterior communication is via the basivertebral venous system (Figure 2.13A–C), which usually forms the largest draining veins from the vertebrae. These veins connect directly to the epidural venous system that surrounds the exiting nerve roots and the thecal sac.

Lateral drainage from the vertebrae communicates to the paravertebral veins. Paravertebral veins form a system along the lateral aspect of the vertebrae running in both vertical and horizontal directions and that interconnect the posterior epidural and anterior central venous elements (Figure 2.13D,E). The central venous elements are large central channels composed of the azygos and caval veins that ultimately return venous blood to the lungs.

Direct entry of cement into the exiting vascular channels is minimized by needle placement away from the majority of these vessels. This risk is highest in the posterior aspect of the vertebra. Lateral and anterior communications are generally much smaller than to the basivertebral plexus (Figure 2.13A). The cement distribution is controlled by least resistance flow. Injecting away from the large (low pressure) channels forces intertrabecular distribution of cement preferentially. Large channels can be encountered accidentally, and continuous observation for this type of cement filling and distribution will limit leaks and prevent serious consequences.

Percutaneous Needle Approaches (Additional Considerations)

Individual needle approaches were generally described above with each segment of the spine for which they are applicable. The transpedicular approach is the most commonly used and provides the safest method of accessing the vertebral body (see Figure 2.8A). This occurs because the pedicle provides a discreet target that is visualized during image-guided needle placement. There are no structures within the pedicle that can be damaged during accurate transpedicular needle insertion. Percutaneous vertebroplasty can be accomplished in 85%–95% of cases using this route, as most compression fractures occur from T6 to L5 and the pedicle structure is adequate for needle insertion throughout this region. Complications that can occur with alternate routes (pneumothorax and bleeding with parapedicular; damage to vascular structures with anterolateral) are avoided with the transpedicular route. It should be the mainstay for needle placement with alternate routes reserved for relatively rare situations.

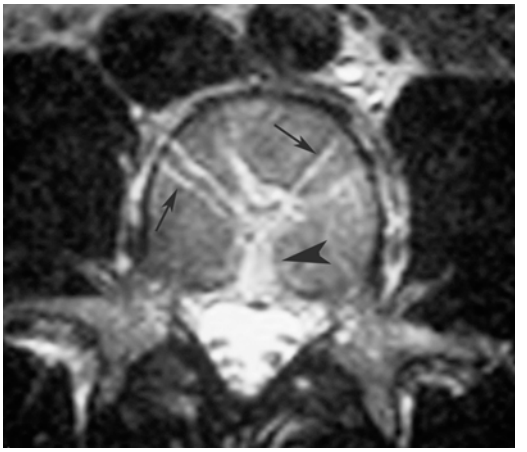

A

B

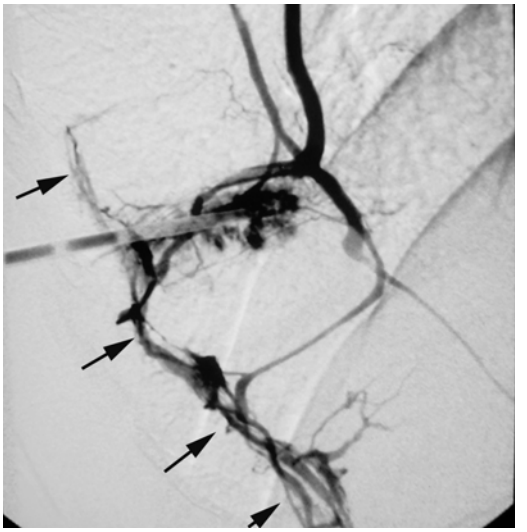

C

D

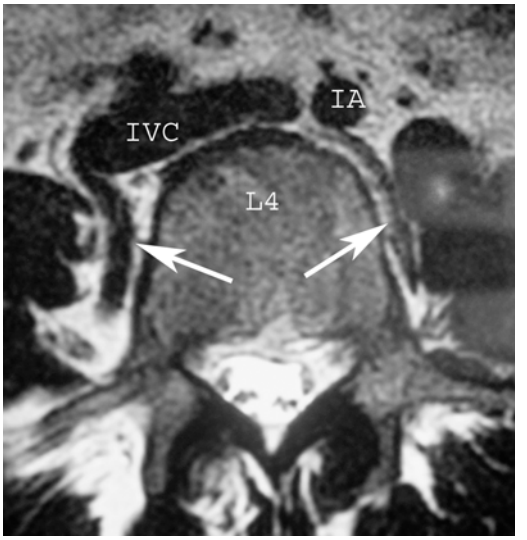

E

The parapedicular route may be used when the pedicle is absent (due to tumor), not seen because of severe osteoporosis, or too small (see Figure 2.8B,C). It does suffer from the potential for pneumothorax or bleeding. Also known as the transcostovertebral needle route, it passes along the rib margin in the thoracic spine. In some patients the lung may bulge beyond the lateral rib margin and put it at risk for pneumothorax. Bleeding may occur to a greater degree than found with the transpedicular approach, as the entry site into bone in the parapedicular approach is along the lateral aspect of the vertebra. Paravertebral arteries and veins run in this location. They can be quite large (Figure 2.13D,E) and are put at risk for puncture or transaction with this needle approach. The needle puncture site can be easily compressed with pressure over the stick site in the transpedicular approach. This is not available for the parapedicular region to help limit bleeding, and therefore puncture of the large lateral vertebral vessels may produce more paraspinous bleeding.

The anterolateral approach is not used much as there is relatively little call for cervical or high thoracic PV. Needle placement can be easily accomplished with fluoroscopy in this approach using manual pressure to move the carotid–jugular complex laterally. Confirmation that the needle has missed the vascular structures, however, may be difficult with fluoroscopy alone. For this reason, CT guidance is commonly used for needle placement with this route. As stated above, the trans-oral route is less optimal than the anterolateral approach, as it is impossible to avoid the potential for bacterial contamination going through the mouth.

Fracture Anatomy

Fractures of the vertebrae and sacrum present with typical patterns that are influenced by the biomechanics of each particular spine element. Most compression fractures of the spine result from primary (age-related) or secondary (drug-related) osteoporosis. Relatively minor trauma or vertebra stress may result in compression fracture. These fractures are referred to as *simple* (as opposed to *burst* or *chance* frac-

Figure 2.13. (A) Axial magnetic resonance image (MRI) demonstrates confluence of vessels at the posterior aspect of the vertebral body (black arrowhead). Vascular channels are much smaller, communicating with the paraspinous regions (black arrows). All of the channels give potential avenues for cement leak during injection. **(B,C)** Lateral intraosseous venograms (C is subtracted) of a lower thoracic vertebra. Posterior epidural vessels communicate over multiple levels (black arrows). There is filling of the lateral (paraspinous) channels and anterior vessels that ultimately communicate with the vena cava and lungs. **(D,E)** Lateral and axial MRI images show the large vessels that lie along the lateral aspect of the vertebral bodies in the paraspinous region (white arrows). These vessels are always at risk of injury with the parapedicular needle approach. IVC, inferior vena cava; IA, intraaortic.

tures, more common in primary trauma and produced without underlying pathologic weakening of the bone). Because three fourths of the body weight is born in the anterior two thirds of the spine, the paradigm of a simple fracture creates compression of the anterior body with sparing of the posterior vertebral wall and posterior elements. The anterior endplate region is compromised more often than the inferior endplate (Figure 2.14A). At times both endplates are compressed (Figure 2.14B). Single vertebral fractures are more common than multiple fractures at any one presentation. There is a general trend of fractures to cluster about T12–L1 and to a lesser degree around T7–T8 (10). Subsequent fracture risk increases by 5–10 times once the first osteoporotic fracture occurs at any site (11). The amount of vertebral height loss is not related to the amount of clinical pain experienced by the patient or to how long pain will last.

Variations on the simple compression fracture are common. There may be compression of the posterior wall with or without buckling of the wall into the spinal canal (Figure 2.14C). Fortunately, even with considerable posterior buckling there is infrequent symptomatic cord or nerve compression. Percutaneous vertebroplasty and KP procedures should be safe in this situation if there are no clinical symptoms of neurologic compromise.

Compression fractures can create a cavity or cleft in the vertebra that can be fluid- or air-filled (Figure 2.15). These cavities fill preferentially with cement during treatment and demonstrate very good pain relief.

Nonunion of vertebral bodies is recognized to occur due to lack of fracture healing or osteonecrosis. This situation will often present with signs of motion (or change in height) of the vertebra during respiration or change in body position (Figure 2.16). These fractures are known to provide good opportunity for height restoration during either PV or KP, and their treatment with bone cement also results in very good pain relief.

Compression of vertebrae can be extreme, with height loss greater than 70% (Figure 2.17A). These cases present technical challenges for percutaneous cement injection. Very severe compression usually cannot be treated with KP, as the instruments are larger than those used for PV. Percutaneous vertebroplasty can be accomplished in some cases, as lateral sparing of the vertebrae (greater central compression) is commonly found (Figure 2.17B). This will allow the surgeon to place bilateral needles for cement injection into the less compressed lateral segments. However, as the vertebra becomes progressively compressed, technically getting the needle into an adequate position in the anterior part of the vertebra becomes more and more difficult. Extreme collapse will force the endplates to be very close together, and therefore the needle trajectory will have to be essentially parallel to the endplates (Figure 2.17C). A steeper angle of the needle with respect to the endplates, acceptable in less compression, will not achieve an adequately anterior location for safe cement injection in the most severe compressions.

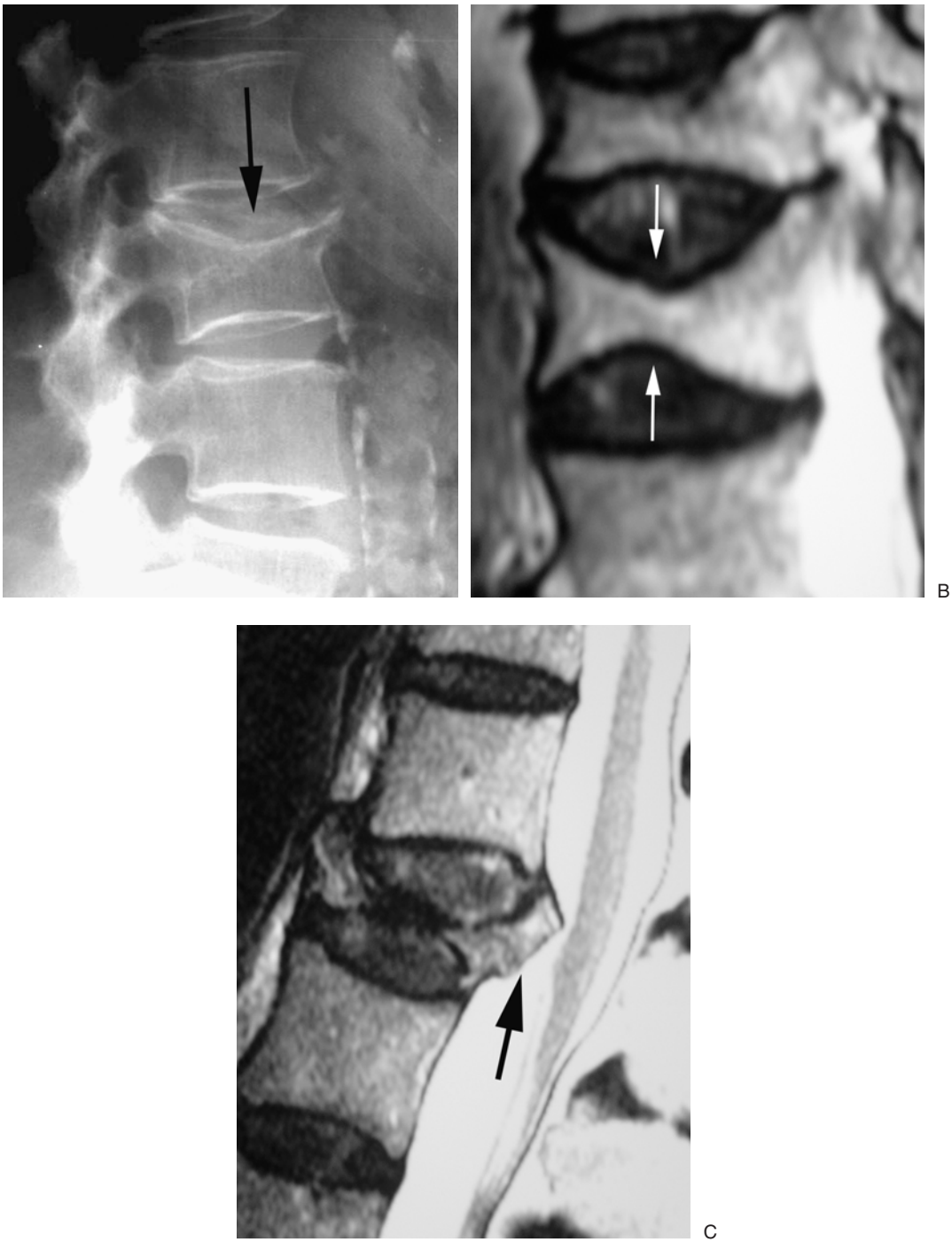

Figure 2.14. (A) Radiograph shows a simple compression fracture. The superior endplate is collapsed (black arrow), with most of the height loss in the anterior vertebrae and general sparing of the posterior wall. **(B)** Sagittal MRI shows a compression fracture with both endplate regions affected (white arrows). **(C)** Sagittal MRI shows marked collapse and buckling of the posterior wall (black arrow). There is mild encroachment on the spinal canal. In this patient there were no symptoms of cord compression and no contraindication to PV based on the canal encroachment.

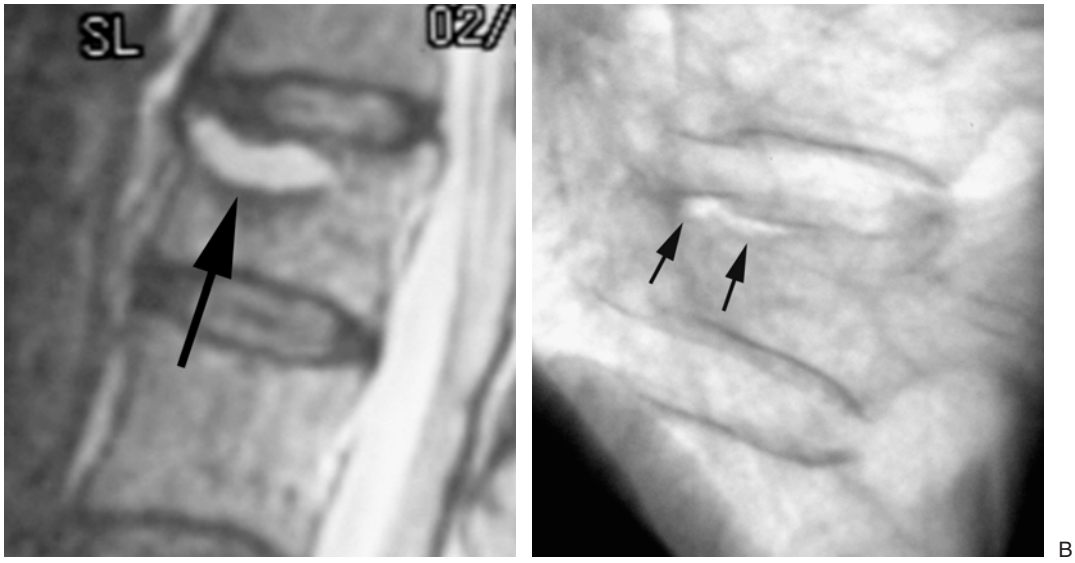

Figure 2.15. (A) Sagittal MRI (T2 weighted) demonstrates a localized region of high signal below the superior endplate (black arrow) that represents a cavity that was formed by the compression injury. **(B)** Lateral radiograph that shows a gas-filled cleft (black arrows) below the superior endplate. This finding is equivalent to the MR findings in A.

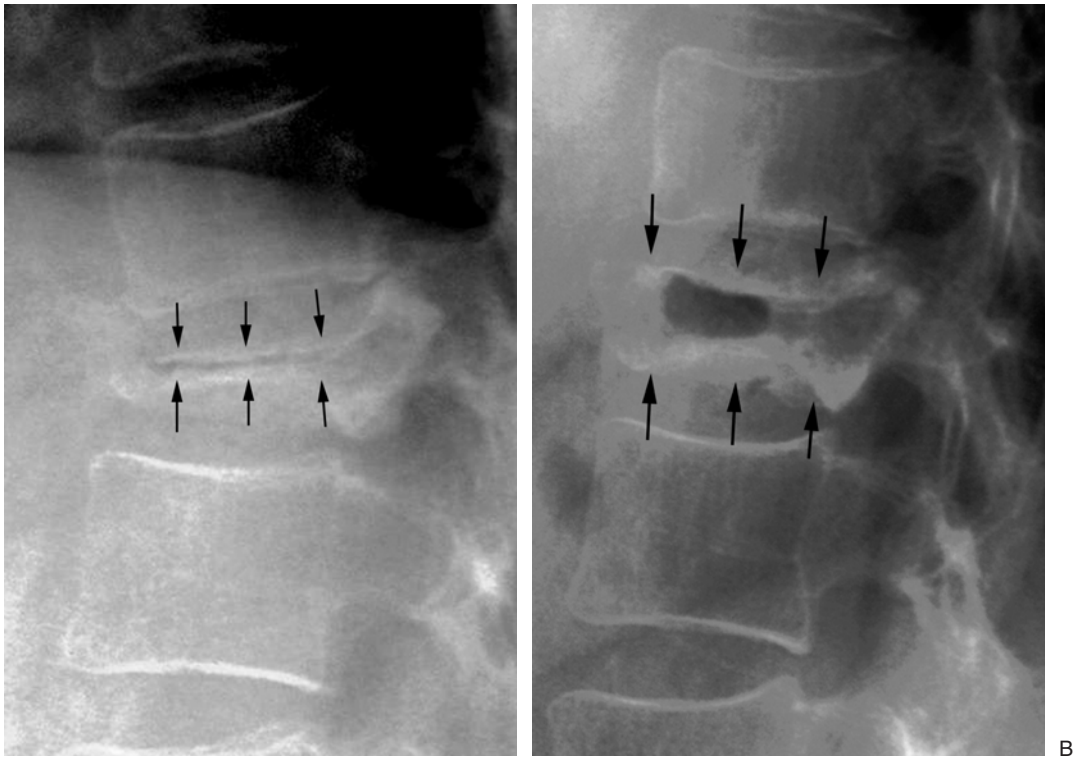

Figure 2.16. (A) Lateral radiograph shows a markedly collapsed vertebral body (black arrows). The patient is standing. **(B)** The mobility of the vertebrae (black arrows) is demonstrated with the patient lying prone. This mobility is consistent with vertebral nonunion. Percutaneous vertebroplasty will recapture the height gained during prone positioning.

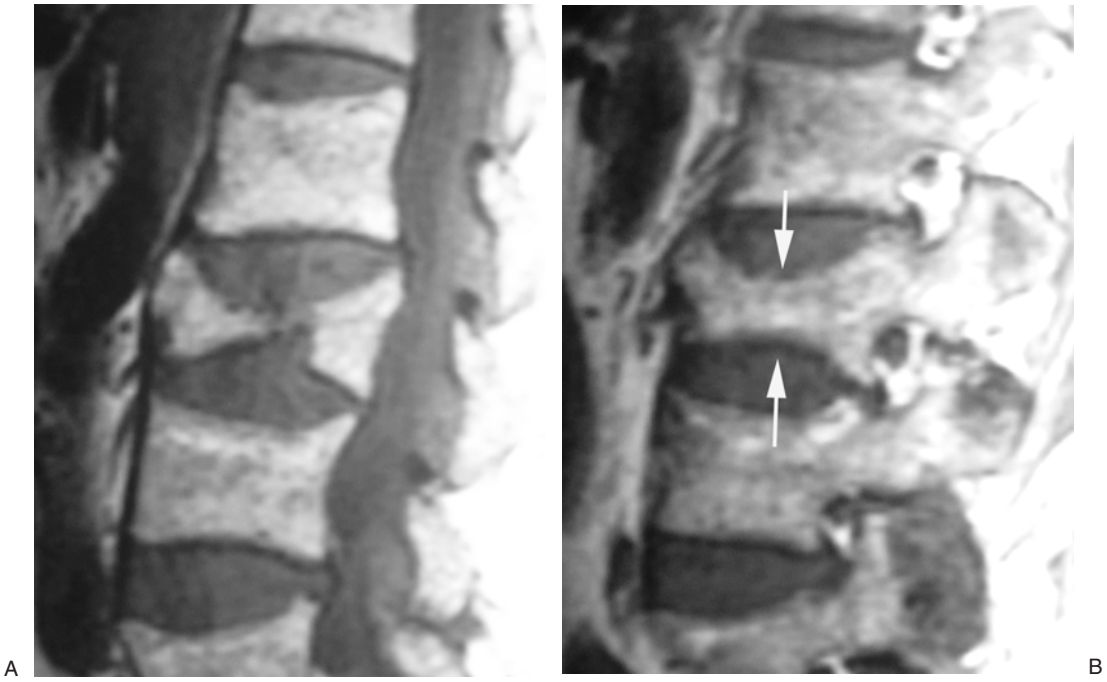

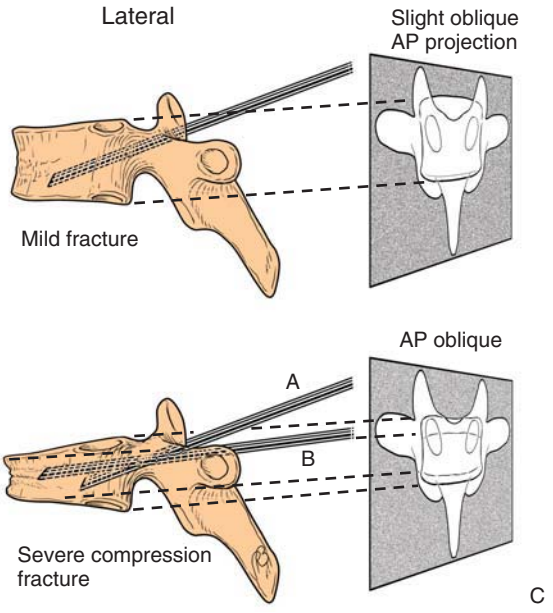

Figure 2.17. **(A)** Sagittal MR image in the midline shows nearly complete collapse of the vertebra centrally. **(B)** A more lateral image of the same patient demonstrates that less compression is present laterally (white arrows). **(C)** With severe compression, a needle angle that is nearly parallel to the endplates **(B)** is required to access the anterior vertebral body. The angle of needle A, acceptable for mild compression, will not work well for extreme compression.

An uncommon presentation is the vertical fractures in which there is literally separation of the anterior and posterior vertebral body (Figure 2.18). These fractures can be treated by "tying" the two halves of the vertebra together with cement. Cement injected in this situation should bridge the fracture site. This is accomplished by achieving an anterior needle location followed by a continuous fill that ties the anterior and posterior portions of the vertebra together.

Although the posterior elements are usually spared with "simple" fractures, there are situations when osteoporotic fractures will involve the posterior elements (Figure 2.19). Cement fixation of the body itself will provide sufficient stabilization in most cases for subsequent healing and pain relief. Injecting cement into fractured pedicles has been described ("pediculoplasty"), but the need for this therapy has not been proved because treatment of the body alone also results in pain relief (12).

Burst and chance fractures are not presently indicated to be appropriate for this procedure, as there are insufficient data to determine whether these fractures can safely be treated with cement injection alone. It has been postulated that first making a cavity (KP) allows a safer method for containing the cement than with

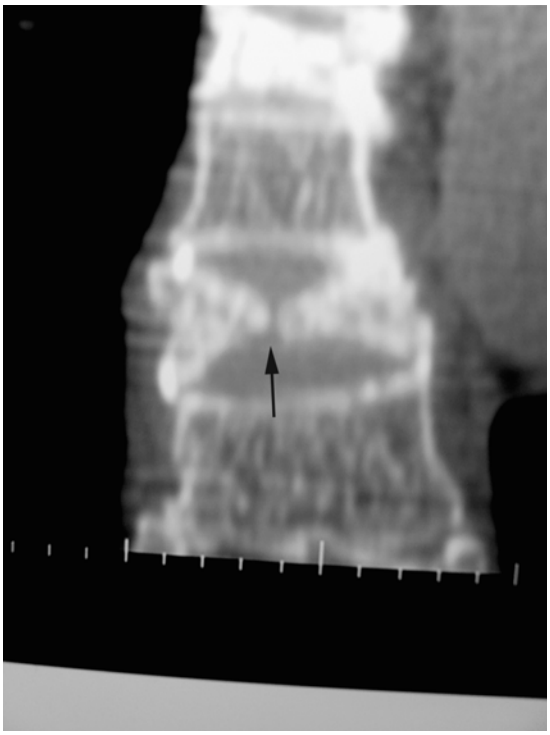

Figure 2.18. A sagittal CT reconstruction demonstrates the vertical fracture that separates the anterior and posterior vertebral body (black arrow).

Figure 2.19. A sagittal MR image shows a fracture line extending into the posterior elements of this vertebra (black arrows). This is a common result in ankylosing spondyolitis.

standard PV. Too few cases are available for the technique to be proved at this time.

Sacral insufficiency fractures are sheer fractures rather than the compression injuries, typical of the vertebral bodies. Sacral insufficiency fractures have characteristic anatomic presentations that are seen well with CT, magnetic resonance imaging, and nuclear scanning, but are not well detected with standard radiographs (Figure 2.20). During fracture, the lateral aspect of the sacral ala sheers away from the central sacral body. These fractures may involve one or both sacral wings, with or without involvement of the central sacrum (Figure 2.21). A fracture of a single wing may progress over time to involve both wings and the central body of the sacrum (Figure 2.22).

Sacral insufficiency fractures are complex and often involve the wall of the neural foramina, which can allow direct cement leakage into this space. The complex anatomy of the sacrum makes cement monitoring difficult with fluoroscopy alone.

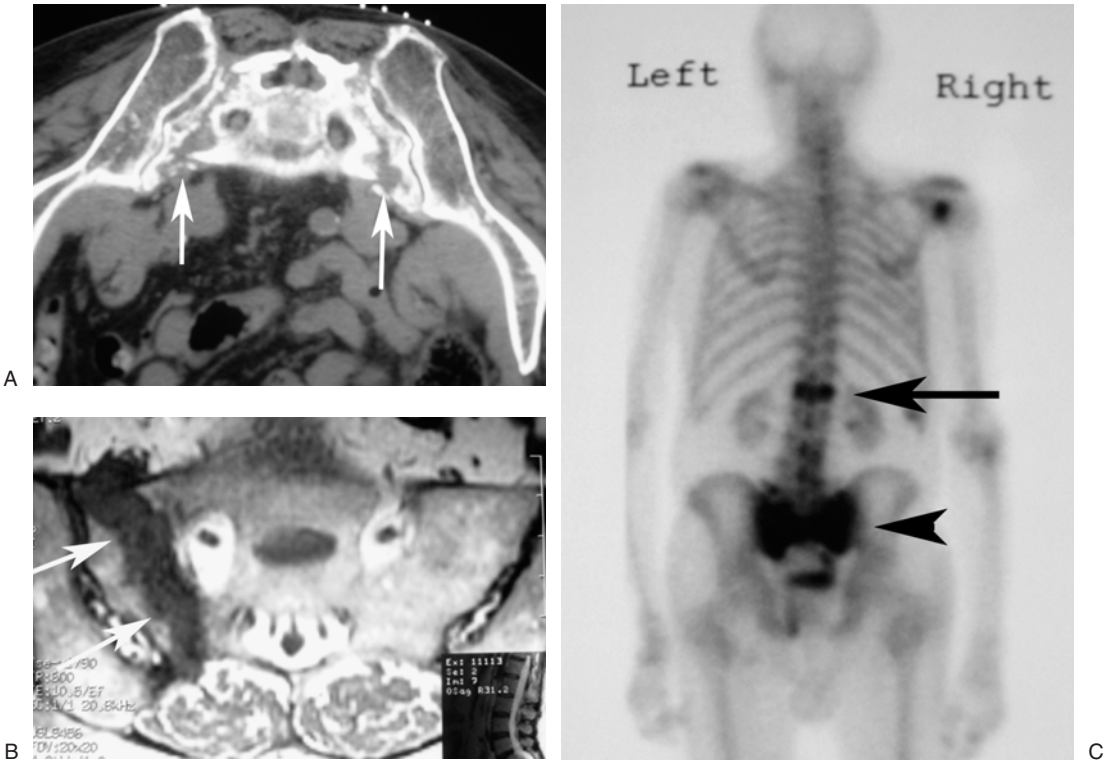

Figure 2.20. **(A)** Axial CT demonstrates bilateral sacral wing fractures (white arrows). **(B)** Coronal T1 MR image shows a unilateral sacral wing fracture (white arrows). The dark signal in the fracture is consistent with marrow edema. **(C)** A bone scan demonstrates a sacral insufficiency fracture (black arrowhead) associated with a vertebral compression fracture (black arrow).

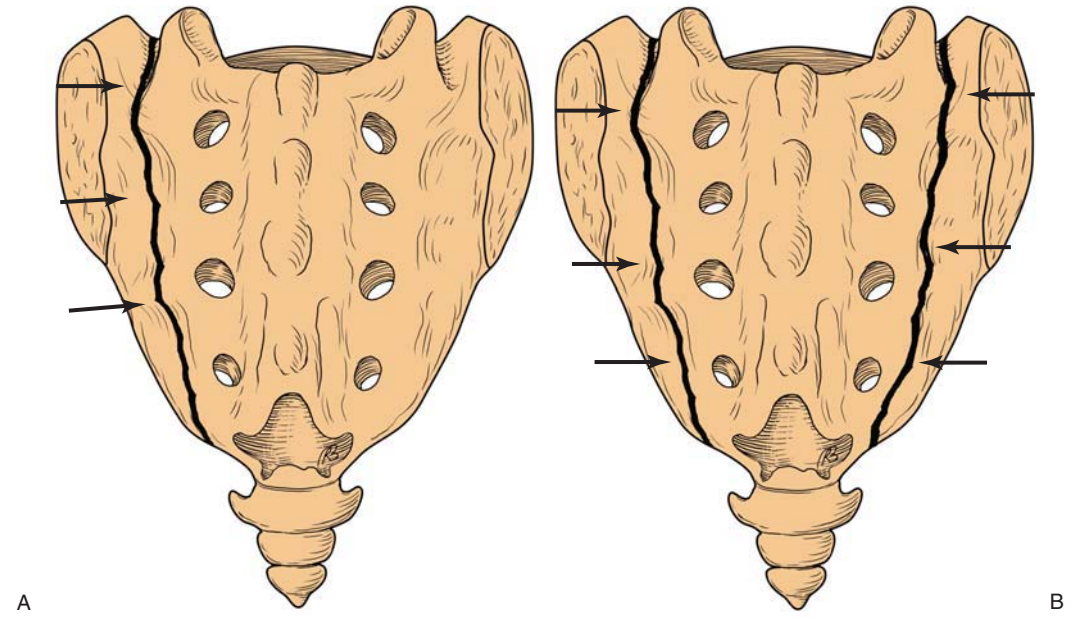

Figure 2.21. **(A)** Drawing of the sacrum demonstrates a unilateral sacral wing fracture (black arrows). **(B)** This drawing shows the bilateral sacral wing fracture (black arrows).

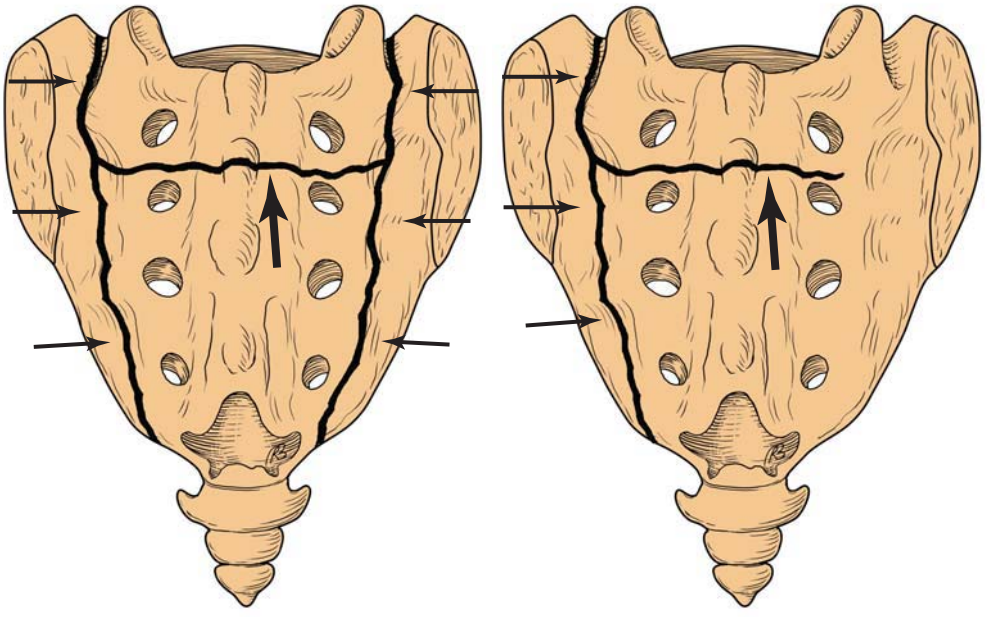

Figure 2.21. *Continued* **(C)** The fracture can extend through the central sacral region (large black arrow) connecting fractures through the lateral alar regions (smaller arrows). **(D)** This drawing shows a fracture limited to one sacral wing and extending into the central sacral body (black arrows). It spares the other sacral wing.

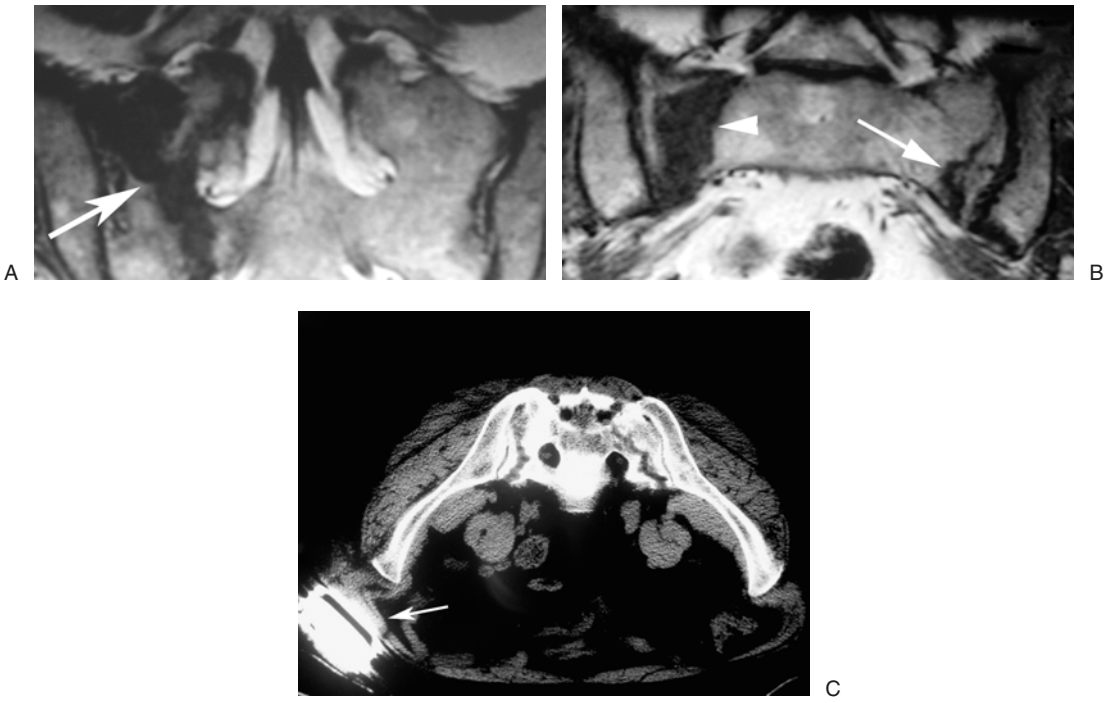

Figure 2.22. **(A)** Coronal T1 MR image shows the initial presenting sacral fracture that involves only one sacral wing (white arrow). **(B)** The same patient 2 months later has a repeat scan that now reveals another fracture extending into the opposite sacral wing (white arrow). The initial fracture (white arrowhead) is still seen. **(C)** A CT scan at the time of treatment with PS demonstrates the bilateral sacral wing fractures. Note that the patient has a pain pump (white arrow) in place and has had disabling pain throughout the course of this 6-month period.

References

1. Ortiz OO, Deramond H. Spine anatomy. In Percutaneous Vertebroplasty, JM Mathis, H Deramond, and SM Belkoff (eds). New York: Springer, 2001: 7–24.
2. Mathis JM, Shaibani A, Wakhloo AK. Spine anatomy. In Image-Guided Spine Interventions, JM Mathis JM (ed). New York: Springer, 2003:1–26.
3. Christenson PC. The radiologic study of the normal spine: cervical, thoracic and lumbar and sacral. Radiol Clin North Am 1977; 15:133–154.
4. Tong FC, Cloft HJ, Joseph GJ, et al. Transoral approach to cervical vertebroplasty for multiple myeloma. Am J Roentgenol 2000; 175:1322–1324.
5. Kothe R, O'Holleran JD, Liu W, et al. Internal architecture of the thoracic pedicle. An anatomic study. Spine 1996; 21:264–270.
6. Brugieres P, Gaston A, Heran F, et al. Percutaneous biopsies of the thoracic spine under CT guidance: transcostovertebral approach. J Comput Assist Tomogr 1990; 14:446–448.
7. Dufresne AC, Brunet E, Sola-Martinez MT, et al. Percutaneous vertebroplasty of the cervico-thoracic junction using an anterior route. J Neuroradiol 1998; 25:123–126.
8. Panjabi MM, Goel V, Oxland T, et al. Human lumbar vertebrae. Quantitative three-dimensional anatomy. Spine 1992; 17:299–306.
9. Lasjaunias P, Berenstein A. Surgical Neuroangiography. New York: Springer, 1990.
10. Nevitt MC, Ross PD, Palermo L, et al. Association of prevalent vertebral fractures, bone density, and alendronate treatment with incident vertebral fractures: effect of number and spinal location of fractures. Bone 1999; 25:613–619.
11. Cooper C, O'Neill T, Silman A. The epidemiology of vertebral fractures. Bone 1993; 14:S89–S97.
12. Eyheremendy EP, De Luca SE, Sanabria E. Percutaneous pediculoplasty in osteoporotic compression fractures. J Vasc Intervent Radiol 2004; 15: 869–874.